$^1O_2$ Generating Luminescent Lanthanide Complexes with 1,8-Naphthalimide-based Sensitizers

Journal:	*Inorganic Chemistry*
Manuscript ID	ic-2019-02431k.R1
Manuscript Type:	Article
Date Submitted by the Author:	28-Aug-2019
Complete List of Authors:	Johnson, Katherine; University of Nevada Reno, Chemistry de Bettencourt-Dias, Ana; University of Nevada Reno, Chemistry

$^{1}O_2$ Generating Luminescent Lanthanide Complexes with 1,8-Naphthalimide-based Sensitizers

*Katherine R. Johnson, Ana de Bettencourt-Dias**

Department of Chemistry, University of Nevada, Reno, NV 89557, United States

ABSTRACT: Lanthanide ion (Ln^{III}) complexes with two new 1,8-naphthalimide-based ligands, **Nap-dpe** and **Nap-cbx**, were isolated and their photophysical properties were explored. Upon excitation at 335 nm, **Nap-dpe** and **Nap-cbx** sensitize visible and near-infrared emitting Ln^{III} ions (Ln^{III} = Eu^{III}, Nd^{III}, and Yb^{III}) and generate singlet oxygen ($^{1}O_2$). Quantum yields of Eu^{III} luminescence for [Eu(**Nap-cbx**)$_3$]$^{3+}$ and [Eu(**Nap-dpe**)$_3$]$^{3+}$ are 17% and 8.3%, respectively, with $^{1}O_2$ generation efficiencies of 41% and 59%, respectively. Efficiencies of $^{1}O_2$ generation for the NIR emitting complexes [Ln(**Nap-dpe**)$_3$]$^{3+}$ are 59% and 56%, respectively, and for [Ln(**Nap-cbx**)$_3$]$^{3+}$ (Ln^{III} = Nd^{III}, Yb^{III}) are 64% and 61%, respectively. In an oxygen-free environment, quantum yields of Eu^{III} luminescence for [Eu(**Nap-cbx**)$_3$]$^{3+}$ and [Eu(**Nap-dpe**)$_3$]$^{3+}$ increase to 20% and 18%, respectively.

INTRODUCTION

Ln^{III} ion luminescence is based on 4*f*-4*f* transitions. Due to shielding of the 4*f* orbitals by the filled 5*s* and 5*p* orbitals, these transitions are not significantly altered by the ion's environment. This leads to characteristic emission with high color purity making luminescent Ln^{III} complexes great candidates for application as imaging agents,[1-2] sensors,[3] anticounterfeiting inks,[4] and in optics.[5-6] However, direct excitation of Ln^{III} ions is inefficient due to the parity-forbidden nature of the *f-f* transitions, which leads to low extinction coefficients. A sensitizer (or antenna) is coordinated to the metal ion to promote Ln^{III}-centered emission, a in a process called the antenna effect.[7] As illustrated in Figure 1, a photon is absorbed by the antenna and generates a ligand-based singlet (^{1}S) excited state. After intersystem crossing (ISC), a triplet (^{3}T) excited state is populated, which then transfers energy to the Ln^{III} excited state. This excited state decays by luminescence. Using an organic ligand as a sensitizer is advantageous because it can be tailored to a specific application or property. For example, our group has isolated several functionalized pybox (pyridine-bis(oxazoline)) ligands that lead to highly-luminescent visible Ln^{III} emitters in organic solvents.[8] When para-functionalized with a glycol tail, the new complexes display efficient luminescence in water,[9] which is valuable for imaging in biological systems.

Our group is now interested in luminescent Ln^{III} complexes with additional properties.[10] As illustrated in Figure 1, the ^{3}T state of the ligand can be used to also generate singlet oxygen ($^1O_2$), a cytotoxic species.[11] Examples of luminescent Ln^{III} compounds capable of generating $^1O_2$ are Tb^{III} DOTA-based complexes functionalized with either naphthyl or azaxanthonyl pendants. These complexes display Tb^{III} emission efficiencies as high as 24% and $^1O_2$ generation efficiencies (ϕ_{1O2}) as high as 12%.[12] Although the complexes are good Tb^{III} sensitizers, their $^1O_2$ generation efficiencies fall well below efficiencies of organic photosensitizers.[13] More recently, Maury and coworkers described a tris-picolinato-1,4-7-triazacyclononane macrocycle with ϕ_{1O2} = 80% when complexed to Gd^{III}. However, when the Gd^{III} ion was exchanged for Yb^{III}, only luminescence was observed, due to the competition between the two energy transfer pathways.[14] This group also recently described helicenic complexes of Ln^{III}, and in this case, good efficiencies of both metal-centered emission and $^1O_2$ generation were observed.[15] As show in Figure 1, the ^3T state is responsible for both generation of $^1O_2$ and Ln^{III} luminescence, and competing non-radiative processes lead to quenching of the excited states. Thus, a good understanding of the interplay between the two properties is important to enable researchers to use compounds with phototoxic properties for therapeutic applications and to track them *in situ* through Ln^{III}-centered luminescence. Thus, we aimed to isolate Ln^{III} complexes that display efficient luminescence and, in addition, efficiently generate $^1O_2$ and chose naphthalimide as the $^1O_2$ generating functional group.

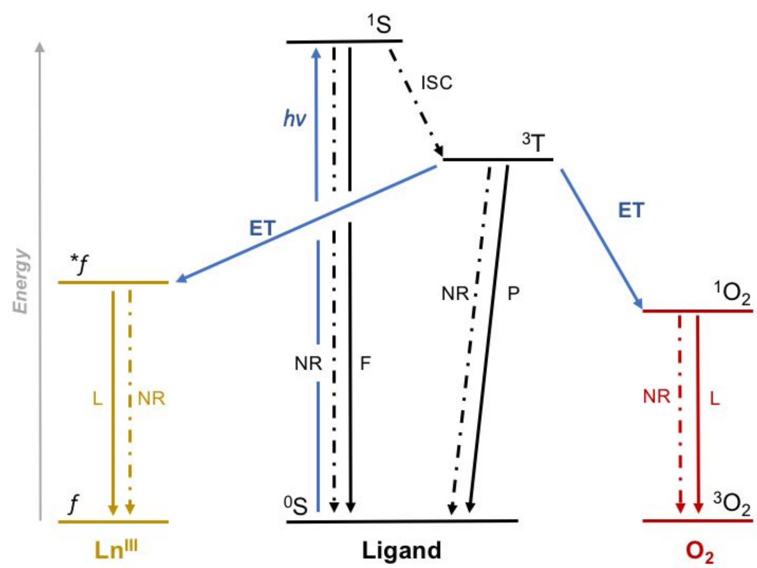

Figure 1. Energy level diagram showing the energy transfer (ET) pathways for both Ln^{III} ion sensitization and $^1O_2$ generation. Energy hν is absorbed by the ligand to populate a singlet excited state (^1S). Intersystem crossing (ISC) leads to population of a triplet excited state (^3T). This state can then transfer energy to populate the emissive **f* excited state which decays by luminescence (L) to the ground state, *f*. Alternatively, the energy transfer leads to $^1O_2$ generation, which decays to triplet oxygen $^3O_2$ by emitting at 1270 nm. Nonradiative (NR) (dash-dot lines) pathways lead to

quenching of excited states. Competing radiative processes are fluorescence (F) and phosphorescence (P). Energy levels are not drawn to scale.

1,8-Naphthalimide is known for its near unit quantum yield of ISC and high quantum yield of $^1O_2$ generation in acetonitrile.[16] 1,8-Naphthalimide-based compounds are also efficient photosensitizers of $^1O_2$, with reported ϕ_{1O2} in the range 5% - 82%,[16-18,19] and are proposed for biological sensing,[20-23] as anti-inflammatory drugs,[24] and as anticancer therapeutics.[25-28] For example, the derivatives amonafide and mitonafide were tested in clinical trials as anticancer agents.[29-30] Naphthalimide and its derivatives intercalate between DNA base pairs and form strong van der Waals interactions,[31] resulting in reduced gene expression.[32] Selected derivatives are reported to bind and disable topoisomerase II (the enzyme responsible for DNA packaging)[33] or tubulin,[34] or nitroreductase,[35] considerably hindering cell function. Naphthalimide derivatives are often used as fluorescent reporters.[17, 24, 26, 36-37] Hideg and co-workers reported an example used to infiltrate chlorophyll-containing mesophyll cells of tobacco leaves, and to detect $^1O_2$ in vitro by luminescence in the range 500 – 600 nm.[38]

1,8-Naphthalimide is easily functionalized,[39] and many groups have investigated ways to increase its potency by adding heavy atoms,[40-41] extending conjugation,[18] or incorporating multiple cytotoxic motifs.[42] Some of these methods do increase the efficiency of ISC but can result in shortening the lifetime of the ^1S excited states. This results in decreased fluorescence efficiency,[18, 40, 43] and thus decreased signal-to-noise ratio,[44] preventing *in situ* and *in vivo* bioimaging. The long-lived luminescence of Ln^{III} ions, which is a result of the forbidden nature of the *f*-*f* transitions, circumvents these two barriers inherent to organic fluorophores.

Luminescent Ln^{III} complexes with 1,8-naphthalimide-based ligands have been reported, but their $^{1}O_2$ generating properties have not been explicitly explored.[6, 45-52] Ward and co-workers studied a Eu^{III} DOTA-based complex featuring a 1,8-naphthalimide pendant that in solution, displays concurrent ligand- and Eu^{III}-centered emission as a white light emitter and they determined a Eu^{III} emission efficiency (ϕ^{Eu}) of 12%.[53] Pischel and co-workers discussed a polyamine-derivatized naphthalimide chromophore for Eu^{III} luminescence with ϕ^{Eu} = 11%.[54] More recently, two 1,8-naphthalimidopyridine-N-oxides were shown to sensitize Eu^{III} luminescence, with ϕ^{Eu} of 42% and 29%.[6]

To expand our knowledge of compounds that generate $^{1}O_2$ and that simultaneously display Ln^{III}-centered luminescence, we isolated two new 1,8-naphthalimide-based compounds, **Nap-dpe** and **Nap-cbx**, shown in Scheme 1, in which a Ln^{III} chelator is present at the imide nitrogen atom. These ligands are easily synthesized, as discussed below, with direct coordination of the two functional groups involved in the sensitization process; this synthetic strategy has proven successful in our group for other families of sensitizers.[55-57] We report here their ability to sensitize Ln^{III} luminescence in the visible and NIR and concurrently generate $^{1}O_2$.

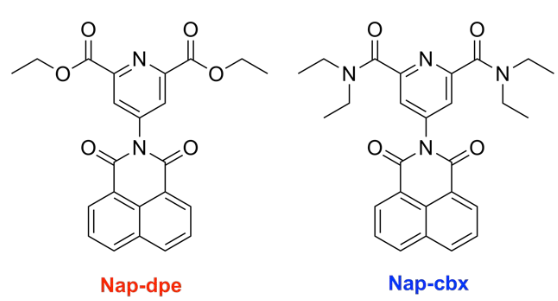

Scheme 1. The compounds **Nap-dpe** and **Nap-cbx** studied here.

RESULTS AND DISCUSSION

Nap-dpe and **Nap-cbx** were synthesized through condensation of 4-aminopyridine-2,6-diethyl ester or 4-aminopyridine-2,6-dicarboxamide with 1,8-naphthalic anhydride in 34% and 46% yields, respectively (Figure S1; details of synthesis can be found in the Supporting Information). We confirmed their isolation by NMR and FT-IR spectroscopy and mass spectrometry (Figures S2 – S8). Both compounds display broad absorption in the ultraviolet (UV) region with maxima at 334 nm. Exciting at ~330 nm results in fluorescence bands with maxima at 380 nm (Figures S9 & S10). Quantum yields of fluorescence (ϕ^F) are 2 and 5% for **Nap-cbx** and **Nap-dpe** (Table 1), respectively, and are similar to other naphthalimide derivatives.[18, 58-60] Upon complexation to Gd^{III}, which cannot be sensitized by these ligands due to its high lying emissive state ($^3P_{7/2}$ at 32,200 cm^{-1}),[61] the emission spectra do not change appreciably (Figures S11 & S12), but a slight red-shift of the emission maxima and an increase in emission efficiency to 6% for [Gd(**Nap-dpe**)$_3$]$^{3+}$ and 7% for [Gd(**Nap-cbx**)$_3$]$^{3+}$ are observed, consistent with planarization of the ligand upon coordination[62] and some phosphorescence contribution, due to improved ISC. In degassed solutions, fluorescence efficiencies increase slightly for all species to ϕ^F = 7% for both **Nap**-based compounds, and 9% for both Gd^{III} complexes, confirming that fluorescence decreases by the simultaneous generation of $^1O_2$ in aerated solution (*vide infra*).

To assess the adequacy of **Nap-dpe** and **Nap-cbx** as sensitizers for Ln^{III} emission, the energies of their singlet (^1S) and triplet (^3T) excited states were determined through fluorescence and phosphorescence spectroscopy of the Gd^{III} complexes (Table 1, Figures S13 – S18).[63] The ^1S and ^3T states are located at 25,700 and 18,300 cm^{-1}, respectively, for [Gd(**Nap-dpe**)$_3$]$^{3+}$ and 26,500 and 21,200 cm^{-1}, respectively, for [Gd(**Nap-cbx**)$_3$]$^{3+}$. As expected, the ^3T excited state for both complexes is lower than what is reported for the ^3T state for chelators diethyl pyridine-2,6-dicarboxylate (23,260 cm^{-1})[64] and N,N,N',N'-tetraethylpyridine-2,6-dicarboxamide (20,600 cm^{-}

^{1})).[65] Using the INDO/S-CIS method[66] and ORCA,[67] as implemented within LUMPAC,[68] we modeled the ground state geometry of the complexes (*vide infra*), as shown in Figure 2. The calculated ^{1}S and ^{3}T excited state energies are 26,231 cm^{-1} and 18,035 cm^{-1} for [Gd(**Nap-dpe**)$_3$]$^{3+}$ and 31,840 cm^{-1} and 21,115 cm^{-1} for [Gd(**Nap-cbx**)$_3$]$^{3+}$ (Table 1), respectively, which compare favorably with the experimental values. These energies indicate that both ligands are capable of sensitizing Eu^{III}, which has its emissive state at 17,300 cm^{-1}, in addition to Yb^{III} and Nd^{III}, with their emissive states at 11,500 cm^{-1} and 11,600 cm^{-1}, respectively.[69-70]

Table 1. Quantum yields of fluorescence (ϕ^{F}) for **Nap-cbx** and **Nap-dpe** and their Gd^{III} complexes and experimental and calculated singlet (^{1}S) and triplet (^{3}T) state energies

Compound	ϕ^{F} [a]	Experimental[b]		Calculated[c]	
	(%)	^{1}S [cm^{-1}]	^{3}T [cm^{-1}]	^{1}S [cm^{-1}]	^{3}T [cm^{-1}]
Nap-cbx	2 ± 0				
	7 ± 1[d]				
Nap-dpe	5 ± 1				
	7 ± 2[d]				
[Gd(**Nap-cbx**)$_3$]$^{3+}$	7 ± 0	26,500 ± 60	21,200± 50	31,840	21,115
	9 ± 1[d]				
[Gd(**Nap-dpe**)$_3$]$^{3+}$	6 ± 0	25,700 ± 150	18,300 ± 10	26,231	18,035
	9 ± 0[d]				

[a]Measured at 25.0 ± 0.1 °C
[b]Measured at 77 K in 1:1 dichloromethane:acetonitrile, reported as the 0 – 0 transition
[c]Calculated using the INDO/S-CIS method[66] and ORCA,[67] as implemented within LUMPAC[68]
[d]Degassed solutions of 1:1 dichloromethane:acetonitrile

The stoichiometry of the complexes in solution was determined through emission titrations of $Eu(NO_3)_3$ with aliquots of either ligand (Figures S19 & S20). The stability constants for the 1:1, 2:1, and 3:1 ligand-to-metal species for the **Nap-dpe** complexes are 8.02 ± 0.07 (log β_1), 14.01 ± 0.24 (log β_2), and 19.00 ± 0.20 (log β_3) and are comparable to the values reported for diethyl pyridine-2,6-dicarboxylate coordinating to Ln^{III}, which are in the range of 6.8 – 7.0 for log β_1, 12.8 – 14.0 for log β_2, and 16.3 – 18.0 for log β_3.[71] Stability constants for the **Nap-cbx** complexes are 8.64 ± 0.12 (log β_1), 14.67 ± 0.11 (log β_2), and 19.80 ± 0.24 (log β_3) (Table S1). These values are similar to the values reported for N,N,N',N'-tetraethylpyridine-2,6-dicarboxamide coordinating to Ln^{III}, which are in the range of 7.3 – 8.5 for log β_1, 13.8 – 16.0 for log β_2, and 21.0 – 22.9 for log β_3.[65] Speciation diagrams for both systems (Figure S21) confirm the presence of the 3:1 complex as the main metal-containing species at the appropriate conditions. The formation of the 3:1 complexes was further assessed through speciation studies using ^{1}H-NMR spectroscopy with the diamagnetic La^{III} analogs (Figures S22 & S23). It is noteworthy that while the speciation diagrams (Figure S21) indicate the possible presence of a small amount of the 2:1 ligand-to-metal ion complex in solution, as discussed below, emission lifetime measurements of the Eu^{III} analogs show that the decay curves can be fit to a single exponential, consistent with the presence of one emissive species in solution.[72-74]

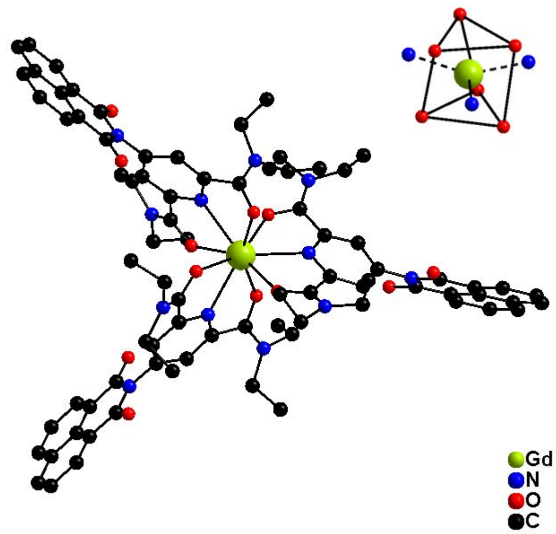

(a)

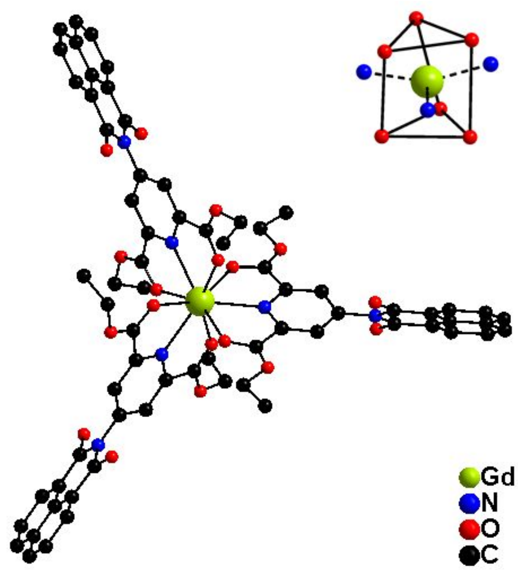

(b)

Figure 2. Ground state geometries of (a) [Gd(**Nap-cbx**)$_3$]$^{3+}$ and (b) [Gd(**Nap-dpe**)$_3$]$^{3+}$. Hydrogen atoms are omitted for clarity. Insets show a tricapped trigonal prismatic coordination geometry around the Gd^{III}.

Attempts to isolate X-ray quality single crystals to confirm structure are ongoing. Nonetheless, the ground state geometry of each complex (Figure 2) was modeled using SPARKLE/PM3[75] implemented in MOPAC2016.[76] In both cases, each Gd^{III} ion is bound to three ligands through the nitrogen atom of the pyridine rings and the carbonyl oxygen atoms of the carboxamide or ester, respectively, resulting in a coordination number of 9. The coordination polyhedra (insets, Figure 2) are, in both cases, distorted tricapped trigonal prisms. To validate the calculated geometry, we compared calculated bond lengths and dihedral angles in these structures with known complexes for which crystallographic data is available. We obtained Gd – N and Gd – O bond distances around 2.5 and 2.6 Å, respectively, for both complexes, similar to what is observed for related dipicolinato-based complexes.[77-78] We calculated dihedral angles between the naphthalimide and pyridyl groups of about ~51 Å, which are comparable to experimental values in similar compounds.[6]

To characterize the photophysical properties of the complexes, [Ln(**Nap-dpe**)$_3$]$^{3+}$ and [Ln(**Nap-cbx**)$_3$]$^{3+}$ were isolated by reacting **Nap-dpe** or **Nap-cbx** with $Ln(NO_3)_3$ (Ln^{III} = Nd^{III}, Eu^{III}, Gd^{III}, and Yb^{III}) in 1:1 dichloromethane:acetonitrile. After filtration and subsequent solvent evaporation, the salts [Ln(**Nap-dpe**)$_3$]$(NO_3)_3$ or [Ln(**Nap-cbx**)$_3$]$(NO_3)_3$ precipitated as white powders in 91 – 98% yield (details in Supporting Information). Their isolation was confirmed through high resolution mass spectrometry (Figures S24 – S31). After redissolving them in 1:1 dichloromethane:acetonitrile, the complexes display the characteristic metal-based emission colors upon excitation. The emission spectra of [Eu(**Nap-cbx**)$_3$]$^{3+}$ and [Eu(**Nap-dpe**)$_3$]$^{3+}$ (Figure 3) show the $^5D_0 \rightarrow {}^7F_J$ ($J = 0 – 4$) transitions of Eu^{III} luminescence. The presence of the $^5D_0 \rightarrow {}^7F_0$ band for both complexes suggests a low symmetry environment around the metal ion.[2] The emission spectra of [Yb(**Nap-cbx**)$_3$]$^{3+}$, [Yb(**Nap-dpe**)$_3$]$^{3+}$, [Nd(**Nap-cbx**)$_3$]$^{3+}$, and [Nd(**Nap-**

dpe)$_3$]$^{3+}$ display the characteristic NIR emission bands for Yb^{III} ($^2F_{5/2} \rightarrow {}^2F_{7/2}$) and Nd^{III} ($^4F_{3/2} \rightarrow {}^4I_J$ (J = 9/2, 11/2, and 13/2)).

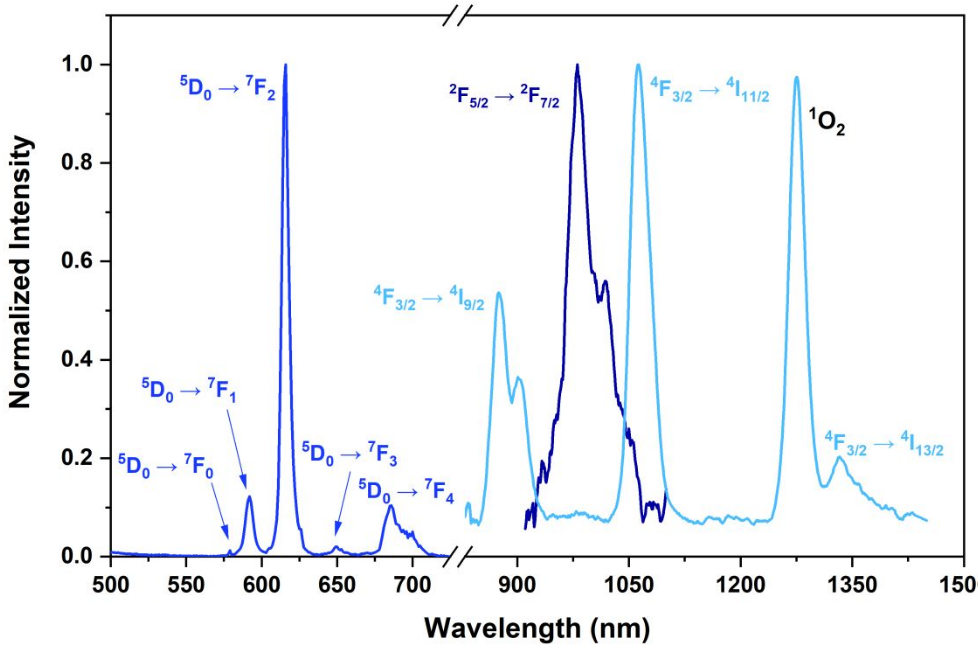

(a)

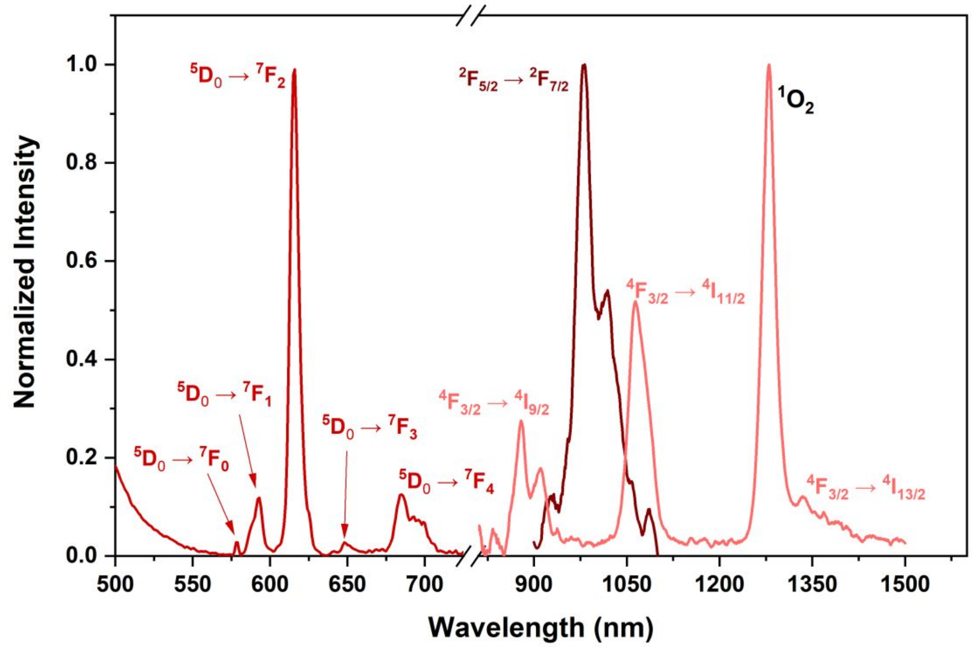

(b)

Figure 3. Normalized emission spectra of the **(a)** [Ln(**Nap-cbx**)$_3$]$^{3+}$ complexes [Ln = Eu^{III} (blue), Nd^{III} (light blue), or Yb^{III}(navy)] and of the **(b)** [Ln(**Nap-dpe**)$_3$]$^{3+}$ complexes [Ln = Eu^{III} (red), Nd^{III} (pink), or Yb^{III}(dark red)] in 1:1 dichloromethane:acetonitrile measured at 25.0 ± 0.1 °C (λ_{exc} = 335 nm).

Quantum efficiencies of sensitized Eu^{III} emission (ϕ^{Eu}) are 8.3% for [Eu(**Nap-dpe**)$_3$]$^{3+}$ and 17% for [Eu(**Nap-cbx**)$_3$]$^{3+}$ (Table 2) and are comparable to reported ϕ^{Eu} for naphthalimide-based complexes (*vide supra*).[53-54] We attribute the lower emission efficiency of [Eu(**Nap-dpe**)$_3$]$^{3+}$ to the narrower gap between the ^{3}T excited state and the emissive $^5D_0$ emissive state,[79] which results in a low sensitization efficiency (η_{sens}) of 38% (Table 2) compared to 52% for [Eu(**Nap-cbx**)$_3$]$^{3+}$, and also explains the residual ligand band seen in the region 500 – 550 nm in the emission spectrum of the former complex (Figure 3b, S32).

The luminescence lifetimes (τ) for both Eu^{III} complexes are 0.51 ms for [Eu(**Nap-dpe**)$_3$]$^{3+}$ and 0.68 ms for [Eu(**Nap-cbx**)$_3$]$^{3+}$ in aerated solution at 298 K. Both τ could be fit as single-exponential decays (Figures S33 & S34, Table S2), indicating one unique coordination environment around the Eu^{III} ions.[72-74] The slightly longer lifetime of [Eu(**Nap-cbx**)$_3$]$^{3+}$ is consistent with a higher intrinsic quantum yield (ϕ^{Eu}_{Eu}= 32%) compared to [Eu(**Nap-dpe**)$_3$]$^{3+}$ (ϕ^{Eu}_{Eu}= 22%) and indicates slightly better shielding from vibrational quenching.[80] In addition, **Nap-dpe** shows slightly lower sensitization efficiency, consistent with the lower energy gap between the ^{3}T state and the $^5D_0$ level of Eu^{III}. Finally, this lower gap leads to a certain degree of back-energy transfer from $^5D_0$ to ^{3}T, as can be seen by the small increase in the emission lifetimes when the solutions of the complexes are cooled to 77 K (Table 2 and Figures S45 and S46, Table S3). This repopulation of the ^{3}T and lower sensitization efficiency are advantageous for a more efficient $^1O_2$ generation for the [Eu(**Nap-dpe**)$_3$]$^{3+}$ complex, as discussed below.

Table 2. The difference in energy (ΔE) between ^{3}T and $^5D_0$ of Eu^{III}, quantum yield of Eu^{III} luminescence (ϕ^{Eu}), observed lifetime (τ), intrinsic quantum yield (ϕ^{Eu}_{Eu}), and sensitization efficiency (η_{sens}) for the Eu^{III} complexes in aerated and degassed solutions.

Compound	ΔE (^{3}T – $^5D_0$) (cm^{-1})	ϕ^{Eu} [%]^a	τ (ms)^a	ϕ^{Eu}_{Eu} [%]	η_{sens} [%]
[Eu(**Nap-dpe**)$_3$]$^{3+}$	~1,000	8.3 ± 0.0 17.7 ± 0.2^b	0.51 ± 0.01; 0.81± 0.02^b 1.08 ± 0.08 ^{d}	22 35^c	38 51^c

[Eu(**Nap-cbx**)$_3$]$^{3+}$	~4,000	16.7 ± 0.1 20.4 ± 0.5^b	0.68 ± 0.01; 0.85 ± 0.03^b 1.10 ± 0.04 ^{d}	32 39^c	52 53^c

^{a} Measured at 25.0 ± 0.1 °C in 1:1 dichloromethane:acetonitrile.
^{b} Degassed 1:1 dichloromethane:acetonitrile
^{c} Calculated from data collected in degassed solutions
^{d} Degassed 1:1 dichloromethane:acetonitrile at 77 K.

Quantum yields of Yb^{III} and Nd^{III} luminescence emission and emission lifetimes could not be determined reliably due to weak emission.

All compounds discussed here generate $^1O_2$. Its formation was evaluated by monitoring the phosphorescence at 1270 nm from the $^1O_2 \rightarrow {}^3O_2$ transition (Figures S35 & S36). The $^1O_2$ generation efficiencies (ϕ_{1O2}) for **Nap-cbx** and **Nap-dpe** are 60% and 56% (Table 3), respectively, comparable to values reported for other naphthalimide derivatives.[16, 18] All metal complexes generate $^1O_2$ with efficiencies comparable to **Nap-cbx** and **Nap-dpe**, as summarized in Table 3. They are 41% for [Eu(**Nap-cbx**)$_3$]$^{3+}$, 59% for [Eu(**Nap-dpe**)$_3$]$^{3+}$, 59% and 56% for [Nd(**Nap-dpe**)$_3$]$^{3+}$ and [Yb(**Nap-dpe**)$_3$]$^{3+}$, respectively, and 64% and 61% for [Nd(**Nap-cbx**)$_3$]$^{3+}$ and [Yb(**Nap-cbx**)$_3$]$^{3+}$, respectively. The largest ϕ_{1O2} are observed for the Gd^{III} complexes which are 72% for [Gd(**Nap-dpe**)$_3$]$^{3+}$ and 68% for [Gd(**Nap-cbx**)$_3$]$^{3+}$. These values are similar to values of ϕ_{1O2} for Gd^{III} complexes reported by Maury and coworkers.[14-15] These values are also similar to a variety of naturally occurring $^1O_2$ photosensitizers, such as clorin-e_6 (64% in phosphate buffer),[81] chlorophyll *a* (44% in ethanol),[82] riboflavin (48% in methanol),[83] porfimer sodium (89% in phosphate buffer),[81] and lutetium texaphyrin (23% in methanol).[84]

Table 3. Quantum yields of singlet oxygen generation (ϕ_{1O2}) at 25.0 ± 0.1 °C in 1:1 dichloromethane:acetonitrile.

Compound	ϕ_{1O2} [%]	Compound	ϕ_{1O2} [%]
Nap-cbx	60 ± 1	**Nap-dpe**	56 ± 2
[Gd(**Nap-cbx**)$_3$]$^{3+}$	68 ± 4	[Gd(**Nap-dpe**)$_3$]$^{3+}$	72 ± 2
[Eu(**Nap-cbx**)$_3$]$^{3+}$	41 ± 5	[Eu(**Nap-dpe**)$_3$]$^{3+}$	59 ± 2
[Nd(**Nap-cbx**)$_3$]$^{3+}$	64 ± 1	[Nd(**Nap-dpe**)$_3$]$^{3+}$	59 ± 5
[Yb(**Nap-cbx**)$_3$]$^{3+}$	61 ± 3	[Yb(**Nap-dpe**)$_3$]$^{3+}$	56 ± 2

As mentioned, all Ln^{III} complexes generate $^1O_2$, while concurrently displaying metal-centered emission, which, while not demonstrated here, should facilitate luminescence imaging. To further characterize the concurrent processes of $^1O_2$ generation and metal-centered luminescence, the emission of Eu^{III}, Nd^{III}, and Yb^{III} in the complexes was evaluated in degassed solutions. For all complexes, luminescence emission intensity increased under anaerobic conditions (Figures S37-S42).[15, 54] In the absence of O_2, we observed an increase of ϕ^{Eu} to 17.7% for [Eu(**Nap-dpe**)$_3$]$^{3+}$ and 20% for [Eu(**Nap-cbx**)$_3$]$^{3+}$ (Table 2), as the ^{3}T state is only involved in sensitization of Eu^{III} emission but not in $^1O_2$ generation.[15, 54] The increased emission intensity also leads to an increase in both Eu^{III} lifetimes to 0.81 and 0.85 ms for [Eu(**Nap-dpe**)$_3$]$^{3+}$ and [Eu(**Nap-cbx**)$_3$]$^{3+}$, respectively (Figures S43 & S44), higher ϕ^{Eu}_{Eu} of 39% for [Eu(**Nap-cbx**)$_3$]$^{3+}$ and 35% for [Eu(**Nap-dpe**)$_3$]$^{3+}$ and higher sensitization efficiencies, η_{sens}, of 53% and 51% for [Eu(**Nap-cbx**)$_3$]$^{3+}$ and [Eu(**Nap-dpe**)$_3$]$^{3+}$, respectively.

Despite the expectation that efficiencies of NIR emission would be larger in degassed solutions, quantum yields of Yb^{III} and Nd^{III} luminescence emission and emission lifetimes under these conditions are still too weak to be determined reliably.

CONCLUSIONS

We isolated two new sensitizing ligands based on 1,8-naphthalimide, **Nap-dpe** and **Nap-cbx**, and their lanthanide compounds then demonstrated their ability to concurrently sensitize Ln^{III}-centered emission in the visible and NIR and generate $^1O_2$ in solution upon excitation at 330 nm. The compounds with the largest $^1O_2$ generation efficiencies while sensitizing Ln^{III} luminescence are [Nd(**Nap-cbx**)$_3$]$^{3+}$ (64%) and [Eu(**Nap-dpe**)$_3$]$^{3+}$ (59%). We identified that the complexes' ability to generate $^1O_2$ efficiently impacts the luminescence efficiency, as is expected, due to the involvement of the ^{3}T excited state of the ligand in both processes. While their lack of solubility in water prevents them from being used for bioimaging and therapy purposes, the work presented here expands our knowledge of compounds display the superior properties of emissive Ln^{III} complexes, while simultaneously generating a cytotoxic species.

EXPERIMENTAL SECTION

All commercially obtained reagents were of analytical grade and were used as received. Solvents were dried and purified by standard methods unless otherwise noted. All synthetic steps were completed under N_2 unless otherwise specified. The detailed synthetic procedures of the ligands and their Ln^{III} complexes are provided in the Supporting Information.

Preparation of $Ln(NO_3)_3$ Solutions. The stock solutions of lanthanide(III) nitrate (Ln = Eu^{III}, Gd^{III}, Nd^{III}, or Yb^{III}) nitrate were prepared by dissolving the nitrate salt in spectroscopic grade 1:1 dichloromethane:acetonitrile. The concentration of the metal was determined by complexometric titration with EDTA (0.01 M) using xylenol orange as indicator.[85]

NMR Spectroscopy. All NMR spectra were recorded on Varian 400 and 500 MHz spectrometers with chemical shifts reported (δ, ppm) in deuterated chloroform ($CDCl_3$) against tetramethylsilane (TMS, 0.00 ppm) at 25.0 ± 0.1 °C.

Infrared Spectroscopy. All FT-IR spectra were measured on a Nicolet 6700 FT-IR in ATIR mode. The IR data for each sample were collected in the range 4000 – 590 cm^{-1}, with 32 scans at 4 cm^{-1} resolution per spectrum. A background correction for CO_2 and H_2O was conducted.

Mass Spectrometry. Electrospray ionization mass spectra (ESI-MS) were collected in positive ion mode on a Waters Micromass ZQ quadrupole in the low-resolution mode for the ligands and on an Agilent model G6230A with a QTOF analyzer in the high-resolution mode for the metal complexes. The samples were prepared by diluting acetonitrile solutions to a concentration of ~1 mg/mL and passing through a 0.2 mm microfilter.

Absorption spectroscopy. Absorption spectra were measured on a Perkin Elmer Lambda 35 spectrometer equipped with deuterium and tungsten halogen lamps (Perkin Elmer) and a concave grating with 1053 lines/mm. The absorption spectra were collected using a scan speed of 480 nm/min in the range 225-600 nm with a photodiode detector. All spectra were background corrected, using solvent as the blank. Spectra of the ligands and their complexes were collected using concentrations between 9.0 x 10^{-5} M and 1.25 x 10^{-4} M.

Speciation studies. For speciation studies using emission spectroscopy, spectra were measured in 1:1 dichloromethane:acetonitrile at 25.0 ± 0.1 °C using a constant concentration of $Eu(NO_3)_3$ (1 x 10^{-4} M. Solutions of the ligand and $Eu(NO_3)_3$ were prepared with stoichiometries between 1:0.25 and 1:3.5 (Eu^{III}:ligand), and their emission spectra measured under the same experimental conditions. The concentration of Eu^{III} in solution remained constant, 1 x 10^{-4} M. Fitting and refinement of the data were performed using HypSpec2014.[86] The speciation diagrams were generated using HySS.[87]

For speciation studies using NMR spectroscopy, solutions of **Nap-dpe** and **Nap-cbx** were prepared in a deuterated solvent mixture (1:1 $CDCl_3$:CD_3CN) with ratios of 0:1, 1:1, 2:1, and 3:1

(La^{III}:**Nap-dpe** or La^{III}:**Nap-cbx**). The concentration of ligand, **Nap-dpe** or **Nap-cbx**, was kept constant at 1 x 10^{-3} M. All NMR spectra were recorded on a Varian 400 spectrometer with chemical shifts reported (δ, ppm) against tetramethylsilane (TMS, 0.00 ppm) at 25.0 ± 0.1 °C.

Excitation and emission spectroscopy. Emission and excitation spectra of **Nap-dpe** and **Nap-cbx** and their Ln^{III} complexes were obtained on a Fluorolog-3 fluorimeter (Horiba FL3-22-iHR550), with 1200 grooves/mm excitation monochromator gratings blazed at 330 nm and 1200 grooves/mm or 600 grooves/mm emission monochromator gratings blazed at 500 nm or 1000 nm for UV-Vis or NIR range, respectively. An ozone-free xenon lamp of 450 W (Ushio) was used as the radiation source. The excitation spectra were corrected for instrumental function and measured between 250 and 600 nm. The emission spectra were measured in the range 350-800 nm using a Hamamatsu 928P detector and in the range 800-1600 nm using a Hamamatsu 5509-73 detector cooled with liquid N_2. All emission spectra were also corrected for instrumental function. The ligands' ^{1}S and ^{3}T energies were obtained at ~77 K by deconvoluting the fluorescence and phosphorescence spectra of the analogous gadolinium complexes into their Franck-Condon progression and are reported as the 0-0 transition.[63] Spectra of the ligands and their complexes were collected using solution concentrations of 9.5 x 10^{-5} M to 1.25 x 10^{-4} M.

Emission efficiency measurements. The emission and $^1O_2$ generation quantum yields of the samples were determined by the dilution method using Equation 1.[88]

$$\phi x = \frac{Grad_x}{Grad_{std}} \times \frac{n_x^2}{n_{std}^2} \times \frac{I_{std}}{I_x} \phi std \quad (1)$$

Grad is the slope of the plot of the emission area as a function of the absorbance, *n* is the refractive index of the solvent (n = 1.3870 was determined experimentally for the acetonitrile/dichloromethane mixture; see below), *I* is the intensity of the excitation source at the excitation wavelength used and ϕ is the quantum yield for sample, *x,* and standard, *std*. All data are the average of at least three independent measurements.

Standards for emission quantum yield measurements were quinine sulfate (ϕ = 55%, 5 × 10^{-6} M in aqueous 0.5 M H_2SO_4),[89] $Cs_3[Eu(dpa)_3]$ (ϕ = 24%, 7.5 × 10^{-5} M in aqueous TRIS/HCl buffer (0.1 M, pH ~7.4))[90-91], and 2,2':5',2''-terthiophene (ϕ = 74%,[92]1 × 10^{-4} M in air-saturated acetonitrile) for ligand and Gd^{III} complex fluorescence, Eu^{III} emission, and $^1O_2$ emission, respectively. The excitation wavelengths for both sample and quantum yield standard were chosen to ensure a linear relationship between the intensity of emitted light and the concentration of the absorbing/emitting species (A ≤0.05). $^1O_2$ emission efficiencies should be determined with both sample and standard in the same solvent, due to different oxygen content in different solvents and $^1O_2$ liftetimes, yet this is not always the case.[92-93] However, the mol fractions of O_2 are not very different, at 0.662 in acetonitrile in acetonitrile and 0.709 in dichloromethane.[94] In addition, $^1O_2$ lifetimes are also very similar, with values of 5.4x10^{-5} s in acetonitrile[95] and 5.5x10^{-5} s in dichloromethane.[94] We used the two slightly different solvent systems due to solubility issues. Nonetheless, determination of the emission efficiency of 2,2':5',2"-terthiophene in 1:1 acetonitrile:dichloromethane yielded a value of 77 ± 3%, experimentally equivalent to the value we used for the standard in acetonitrile, and within the range 65 – 81% reported by different authors for this standard in a variety of solvents.[92-93, 96-97]

The intrinsic quantum yield ϕ_{Eu}^{Eu} was determined using equation 2.[98]

$$\phi_{Eu}^{Eu} = \frac{A_{rad}}{A_{tot}} \qquad (2)$$

A_{tot} is the total emission rate ($A_{tot} = k_R + k_{NR} = 1/\tau_{exp}$), where k_R is the radiative rate constant, k_{NR} is the non-radiative decay constant, τ_{exp} is the observed excited state lifetime, and A_{rad} is the radiative emission rate, determined using equation (3).

$$A_{rad} = A_{MD,0} \times n^3 \left(\frac{I_{tot}}{I_{MD}} \right) \qquad (3)$$

I_{tot} and I_{MD} are the total integrated emission spectrum and the area of the $^5D_0 \rightarrow {}^7F_1$ transition, respectively, and $A_{MD,0}$ is Einstein coefficient of spontaneous emission ($A_{MD,0}$ = 14.65 s^{-1}).[99]

The sensitization efficiency (η_{sens}) was determined using equation 4.[98]

$$\eta_{sens} = \frac{\phi^{Eu}}{\phi^{Eu}_{Eu}} \qquad (4)$$

ϕ^{Eu} is the efficiency or quantum yield of sensitized emission.

Refractive Index Measurements. Refractive indices were measured on a Leica MARK II ABBE refractometer with a built-in light source for the measuring prism with an accuracy of ±0.0001 in n_D mode at 25.0 ± 0.2 °C. The average value of three independent measurements (1.3870 ± 0.0004) was used in determining the quantum yield as the refractive index for a 1:1 acetonitrile:dichloromethane solution. This value is in agreement with the value reported by Tsierkezos.[100]

Ground-State Geometries and Excited State Calculations. The Sparkle/PM3 model was used to determine the complexes' ground state geometries.[75] In this model the lanthanide ion is replaced by a +3e point charge.[101] The RHF wave functions were optimized using the Broyden-Fletcher-Goldfarc-Shanno (BFGS) procedure with a convergence criterion of 0.15 kcal/mol*Å and the semi empirical PM3 with a convergence criterion of 10^{-6-} kcal/mol for the SCF. In the MOPAC2016 package[76] the keywords GNORM=0.25, PRECISE, GEO-OK, XYZ, T=10D, and ALLVEC were used. The excited state calculations were preformed using ORCA software[67] using the INDO/S-CIS[66] method.

ASSOCIATED CONTENT

Supporting Information.
The Supporting Information is available free of charge on the ACS Publications website.

AUTHOR INFORMATION

Corresponding Author

*E-mail: abd@unr.edu

ORCID

Ana de Bettencourt-Dias: 0000-0001-5162-2393
Katherine R. Johnson: 0000-0002-1323-0222

Notes

The authors declare no competing financial interest.

ACKNOWLEDGMENTS

Financial support of this work through the National Science Foundation is gratefully acknowledged (Grant CHE 1800392).

REFERENCES

1. Martinić, I.; Eliseeva, S. V.; Nguyen, T. N.; Pecoraro, V. L.; Petoud, S., Near-Infrared Optical Imaging of Necrotic Cells by Photostable Lanthanide-Based Metallacrowns. *J. Am. Chem. Soc.* **2017,** *139*, 8388-8391.

2. Monteiro, J. H. S. K.; Machado, D.; de Hollanda, L. M.; Lancellotti, M.; Sigoli, F. A.; de Bettencourt-Dias, A., Selective Cytotoxicity and Luminescence Imaging of Cancer Cells with a Dipicolinato-based EuIII Complex. *Chem. Commun.* **2017,** *53*, 11818-11821.
3. Xiao, Y.; Ye, Z.; Wang, G.; Yuan, J., A Ratiometric Luminescence Probe for Highly Reactive Oxygen Species Based on Lanthanide Complexes. *Inorg. Chem.* **2012,** *51*, 2940-2946.
4. Andres, J.; Hersch, R. D.; Moser, J.-E.; Chauvin, A.-S., A New Anti-Counterfeiting Feature Relying on Invisible Luminescent Full Color Images Printed with Lanthanide-Based Inks. *Adv. Funct. Mater.* **2014,** *24*, 5029-5036.
5. Tigaa, R. A.; Aerken, X.; Fuchs, A.; de Bettencourt-Dias, A., Sensitization of LnIII (Ln = Eu, Tb, Tm) Ion Luminescence by Functionalized Polycarbonate-Based Materials and White Light Generation. *Eur. J. Inorg. Chem.* **2017**, 5310-5317.
6. Wang, Z.; Liu, N.; Li, H.; Chen, P.; Yan, P., The Role of Blue-Emissive 1,8-Naphthalimidopyridine N-Oxide in Sensitizing EuIII Photoluminescence in Dimeric Hexafluoroacetylacetonate Complexes. *Eur. J. Inorg. Chem.* **2017**, 2211-2219.
7. Weissman, S. I., Intramolecular Energy Transfer The Fluorescence of Complexes of Europium. *J. Chem. Phys.* **1942,** *10*, 214-217.
8. de Bettencourt-Dias, A.; Barber, P. S.; Viswanathan, S.; de Lill, D. T.; Rollett, A.; Ling, G.; Altun, S., Para-Derivatized Pybox Ligands As Sensitizers in Highly Luminescent Ln(III) Complexes. *Inorg. Chem.* **2010,** *49*, 8848-8861.
9. de Bettencourt-Dias, A.; Barber, P. S.; Bauer, S., A Water-Soluble Pybox Derivative and Its Highly Luminescent Lanthanide Ion Complexes. *J. Am. Chem. Soc.* **2012,** *134*, 6987-6994.
10. Monteiro, J. H. S. K.; Sigoli, F. A.; de Bettencourt-Dias, A., A water-soluble TbIII complex as a temperature-sensitive luminescent probe. *Can. J. Chem.* **2017,** *96*, 859-864.
11. Schweitzer, C.; Schmidt, R., Physical Mechanisms of Generation and Deactivation of Singlet Oxygen. *Chem. Rev.* **2003,** *103*, 1685-1758.
12. Law, G.-L.; Pal, R.; Palsson, L. O.; Parker, D.; Wong, K.-L., Responsive and reactive terbium complexes with an azaxanthone sensitiser and one naphthyl group: applications in ratiometric oxygen sensing in vitro and in regioselective cell killing. *Chem. Commun.* **2009**, 7321-7323.
13. Redmond, R. W.; Gamlin, J. N., A Compilation of Singlet Oxygen Yields from Biologically Relevant Molecules. *Photochem. Photobiol.* **1999,** *70*, 391-475.
14. Galland, M.; Le Bahers, T.; Banyasz, A.; Lascoux, N.; Duperray, A.; Grichine, A.; Tripier, R.; Guyot, Y.; Maynadier, M.; Nguyen, C.; Gary-Bobo, M.; Andraud, C.; Monnereau, C.; Maury, O., A “Multi-Heavy-Atom” Approach toward Biphotonic Photosensitizers with Improved Singlet-Oxygen Generation Properties. *Chem.: Eur. J* **2019,** *0*.
15. Galland, M.; Riobé, F.; Ouyang, J.; Saleh, N.; Pointillart, F.; Dorcet, V.; Le Guennic, B.; Cador, O.; Crassous, J.; Andraud, C.; Monnereau, C.; Maury, O., Helicenic Complexes of Lanthanides: Influence of the f-Element on the Intersystem Crossing Efficiency and

Competition between Luminescence and Oxygen Sensitization. *Eur. J. Inorg. Chem.* **2019,** *2019*, 118-125.
16. Aveline, B. M.; Matsugo, S.; Redmond, R. W., Photochemical Mechanisms Responsible for the Versatile Application of Naphthalimides and Naphthaldiimides in Biological Systems. *J. Am. Chem. Soc.* **1997,** *119*, 11785-11795.
17. Liu, X.; Qiao, Q.; Tian, W.; Liu, W.; Chen, J.; Lang, M. J.; Xu, Z., Aziridinyl Fluorophores Demonstrate Bright Fluorescence and Superior Photostability by Effectively Inhibiting Twisted Intramolecular Charge Transfer. *J. Am. Chem. Soc.* **2016,** *138*, 6960-6963.
18. Zhang, L.; Huang, Z.; Dai, D.; Xiao, Y.; Lei, K.; Tan, S.; Cheng, J.; Xu, Y.; Liu, J.; Qian, X., Thio-bisnaphthalimides as Heavy-Atom-Free Photosensitizers with Efficient Singlet Oxygen Generation and Large Stokes Shifts: Synthesis and Properties. *Org. Lett.* **2016,** *18*, 5664-5667.
19. Zhang, L.; Lei, K.; Zhang, J.; Song, W.; Zheng, Y.; Tan, S.; Gao, Y.; Xu, Y.; Liu, J.; Qian, X., One Small Molecule as a Theranostic Agent: Naphthalimide Dye for Subcellular Fluorescence Localization and Photodynamic Therapy In Vivo. *MedChemComm* **2016,** *7*, 1171-1175.
20. Lv, X.; Feng, L.; Ai, C.-Z.; Hou, J.; Wang, P.; Zou, L.-W.; Cheng, J.; Ge, G.-B.; Cui, J.-N.; Yang, L., A Practical and High-Affinity Fluorescent Probe for Uridine Diphosphate Glucuronosyltransferase 1A1: A Good Surrogate for Bilirubin. *J. Med. Chem.* **2017,** *60*, 9664-9675.
21. Su, F.; Agarwal, S.; Pan, T.; Qiao, Y.; Zhang, L.; Shi, Z.; Kong, X.; Day, K.; Chen, M.; Meldrum, D.; Kodibagkar, V. D.; Tian, Y., Multifunctional PHPMA-Derived Polymer for Ratiometric pH Sensing, Fluorescence Imaging, and Magnetic Resonance Imaging. *ACS Appl. Mater. Interfaces* **2018,** *10*, 1556-1565.
22. Sidhu, J. S.; Singh, A.; Garg, N.; Singh, N., Carbon Dot Based, Naphthalimide Coupled FRET Pair for Highly Selective Ratiometric Detection of Thioredoxin Reductase and Cancer Screening. *ACS Appl. Mater. Interfaces* **2017,** *9*, 25847-25856.
23. Lozano-Torres, B.; Galiana, I.; Rovira, M.; Garrido, E.; Chaib, S.; Bernardos, A.; Muñoz-Espín, D.; Serrano, M.; Martínez-Máñez, R.; Sancenón, F., An OFF–ON Two-Photon Fluorescent Probe for Tracking Cell Senescence in Vivo. *J. Am. Chem. Soc.* **2017,** *139*, 8808-8811.
24. Lee, M. H.; Jeon, H. M.; Han, J. H.; Park, N.; Kang, C.; Sessler, J. L.; Kim, J. S., Toward a Chemical Marker for Inflammatory Disease: A Fluorescent Probe for Membrane-Localized Thioredoxin. *J. Am. Chem. Soc.* **2014,** *136*, 8430-8437.
25. Wu, X.; Sun, X.; Guo, Z.; Tang, J.; Shen, Y.; James, T. D.; Tian, H.; Zhu, W., In Vivo and in Situ Tracking Cancer Chemotherapy by Highly Photostable NIR Fluorescent Theranostic Prodrug. *J. Am. Chem. Soc.* **2014,** *136*, 3579-3588.

26. Hettiarachchi, S. U.; Prasai, B.; McCarley, R. L., Detection and Cellular Imaging of Human Cancer Enzyme Using a Turn-On, Wavelength-Shiftable, Self-Immolative Profluorophore. *J. Am. Chem. Soc.* **2014,** *136*, 7575-7578.
27. Dai, F.; Li, Q.; Wang, Y.; Ge, C.; Feng, C.; Xie, S.; He, H.; Xu, X.; Wang, C., Design, Synthesis, and Biological Evaluation of Mitochondria-Targeted Flavone–Naphthalimide–Polyamine Conjugates with Antimetastatic Activity. *J. Med. Chem.* **2017,** *60*, 2071-2083.
28. Lee, M. H.; Kim, J. Y.; Han, J. H.; Bhuniya, S.; Sessler, J. L.; Kang, C.; Kim, J. S., Direct Fluorescence Monitoring of the Delivery and Cellular Uptake of a Cancer-Targeted RGD Peptide-Appended Naphthalimide Theragnostic Prodrug. *J. Am. Chem. Soc.* **2012,** *134*, 12668-12674.
29. Brana, M. F.; Ramos, A., Naphthalimides as Anticancer Agents: Synthesis and Biological Activity. *Curr. Med. Chem. - Anti-Cancer Agents* **2001,** *1*, 237-255.
30. Hsiang, Y. H.; Jiang, J. B.; Liu, L. F., Topoisomerase II-mediated DNA cleavage by amonafide and its structural analogs. *Mol. Pharmacol.* **1989,** *36*, 371.
31. Li, Q.; Browne, W. R.; Roelfes, G., DNA Cleavage Activity of Fe(II)N4Py under Photo Irradiation in the Presence of 1,8-Naphthalimide and 9-Aminoacridine: Unexpected Effects of Reactive Oxygen Species Scavengers. *Inorg. Chem.* **2011,** *50*, 8318-8325.
32. Banerjee, S.; Veale, E. B.; Phelan, C. M.; Murphy, S. A.; Tocci, G. M.; Gillespie, L. J.; Frimannsson, D. O.; Kelly, J. M.; Gunnlaugsson, T., Recent advances in the development of 1,8-naphthalimide based DNA targeting binders, anticancer and fluorescent cellular imaging agents. *Chem. Soc. Rev.* **2013,** *42*, 1601-1618.
33. Chen, Z.; Liang, X.; Zhang, H.; Xie, H.; Liu, J.; Xu, Y.; Zhu, W.; Wang, Y.; Wang, X.; Tan, S.; Kuang, D.; Qian, X., A New Class of Naphthalimide-Based Antitumor Agents That Inhibit Topoisomerase II and Induce Lysosomal Membrane Permeabilization and Apoptosis. *J. Med. Chem.* **2010,** *53*, 2589-2600.
34. Joshi, R.; Mukherjee, D. D.; Chakrabarty, S.; Martin, A.; Jadhao, M.; Chakrabarti, G.; Sarkar, A.; Ghosh, S. K., Unveiling the Potential of Unfused Bichromophoric Naphthalimide To Induce Cytotoxicity by Binding to Tubulin: Breaks Monotony of Naphthalimides as Conventional Intercalators. *J. Phys. Chem. B* **2018,** *122*, 3680-3695.
35. Fang, Y.; Shi, W.; Hu, Y.; Li, X.; Ma, H., A dual-function fluorescent probe for monitoring the degrees of hypoxia in living cells via the imaging of nitroreductase and adenosine triphosphate. *Chem. Commun.* **2018,** *54*, 5454-5457.
36. Zhang, L.; Duan, D.; Liu, Y.; Ge, C.; Cui, X.; Sun, J.; Fang, J., Highly Selective Off–On Fluorescent Probe for Imaging Thioredoxin Reductase in Living Cells. *J. Am. Chem. Soc.* **2014,** *136*, 226-233.
37. Cai, Y.; Guo, Z.; Chen, J.; Li, W.; Zhong, L.; Gao, Y.; Jiang, L.; Chi, L.; Tian, H.; Zhu, W.-H., Enabling Light Work in Helical Self-Assembly for Dynamic Amplification of Chirality with Photoreversibility. *J. Am. Chem. Soc.* **2016,** *138*, 2219-2224.
38. Kalai, T.; Hideg, E.; Ayaydin, F.; Hideg, K., Synthesis and potential use of 1,8-naphthalimide type 1O2 sensor molecules. *Photochem. Photobiol. Sci.* **2013,** *12*, 432-438.

39. Prévost, S.; Dezaire, A.; Escargueil, A., Intramolecular Aryne-Furan Cycloadditions for the Synthesis of Anticancer Naphthalimides. *J. Org. Chem.* **2018,** *83*, 4871-4881.
40. Yogo, T.; Urano, Y.; Ishitsuka, Y.; Maniwa, F.; Nagano, T., Highly Efficient and Photostable Photosensitizer Based on BODIPY Chromophore. *J. Am. Chem. Soc.* **2005,** *127*, 12162-12163.
41. Ryan, G. J.; Quinn, S.; Gunnlaugsson, T., Highly Effective DNA Photocleavage by Novel "Rigid" Ru(bpy)3-4-nitro- and -4-amino-1,8-naphthalimide Conjugates. *Inorg. Chem.* **2008,** *47*, 401-403.
42. Pina, J.; Seixas de Melo, J. S., A comprehensive investigation of the electronic spectral and photophysical properties of conjugated naphthalene-thiophene oligomers. *Phys. Chem. Chem. Phys.* **2009,** *11*, 8706-8713.
43. Rangasamy, S.; Ju, H.; Um, S.; Oh, D.-C.; Song, J. M., Mitochondria and DNA Targeting of 5,10,15,20-Tetrakis(7-sulfonatobenzo[b]thiophene) Porphyrin-Induced Photodynamic Therapy via Intrinsic and Extrinsic Apoptotic Cell Death. *J. Med. Chem.* **2015,** *58*, 6864-6874.
44. Cho, U.; Riordan, D. P.; Ciepla, P.; Kocherlakota, K. S.; Chen, J. K.; Harbury, P. B., Ultrasensitive optical imaging with lanthanide lumiphores. *Nat. Chem. Biol.* **2017**, 15-21.
45. Reger, D. L.; Leitner, A. P.; Smith, M. D., Supramolecular Metal–Organic Frameworks of s- and f-Block Metals: Impact of 1,8-Naphthalimide Functional Group. *Crys. Growth Des.* **2016,** *16*, 527-536.
46. Bonnet, C. S.; Devocelle, M.; Gunnlaugsson, T., Luminescent lanthanide-binding peptides: sensitising the excited states of Eu(iii) and Tb(iii) with a 1,8-naphthalimide-based antenna. *Org. Biomol. Chem* **2012,** *10*, 126-133.
47. Reger, D. L.; Leitner, A.; Smith, M. D., Homochiral, Helical Coordination Complexes of Lanthanides(III) and Mixed-Metal Lanthanides(III): Impact of the 1,8-Naphthalimide Supramolecular Tecton on Structure, Magnetic Properties, and Luminescence. *Crys. Growth Des.* **2015,** *15*, 5637-5644.
48. Zhang, J.; Li, H.; Chen, P.; Sun, W.; Gao, T.; Yan, P., A new strategy for achieving white-light emission of lanthanide complexes: effective control of energy transfer from blue-emissive fluorophore to Eu(iii) centres. *J. Mater. Chem. C* **2015,** *3*, 1799-1806.
49. Carter, A. B.; Zhang, N.; Kühne, I. A.; Keene, T. D.; Powell, A. K.; Kitchen, J. A., Layered Ln(III) Complexes from a Sulfonate-Based 1,8-Naphthalimide: Structures, Magnetism and Photophysics. *ChemistrySelect* **2019,** *4*, 1850-1856.
50. Alcala, M. A.; Shade, C. M.; Uh, H.; Kwan, S. Y.; Bischof, M.; Thompson, Z. P.; Gogick, K. A.; Meier, A. R.; Strein, T. G.; Bartlett, D. L.; Modzelewski, R. A.; Lee, Y. J.; Petoud, S.; Brown, C. K., Preferential accumulation within tumors and in vivo imaging by functionalized luminescent dendrimer lanthanide complexes. *Biomaterials* **2011,** *32*, 9343-9352.

51. Liu, W.; Chen, C.; Huang, X.; Xie, E.; Liu, W., Functional construction of dual-emitting 4-aminonaphthalimide encapsulated lanthanide MOFs composite for ratiometric temperature sensing. *Chem.: Eur. J* **2019,** *0*.
52. Plyusnin, V. F.; Kupryakov, A. S.; Grivin, V. P.; Shelton, A. H.; Sazanovich, I. V.; Meijer, A. J. H. M.; Weinstein, J. A.; Ward, M. D., Photophysics of 1,8-naphthalimide/Ln(iii) dyads (Ln = Eu, Gd): naphthalimide [rightward arrow] Eu(iii) energy-transfer from both singlet and triplet states. *Photochem. Photobiol.* **2013,** *12*, 1666-1679.
53. Shelton, A. H.; Sazanovich, I. V.; Weinstein, J. A.; Ward, M. D., Controllable Three-component Luminescence from a 1,8-naphthalimide/Eu(iii) Complex: White Light Emission from a Single Molecule. *Chem. Commun.* **2012,** *48*, 2749-2751.
54. de Sousa, M.; Kluciar, M.; Abad, S.; Miranda, M. A.; de Castro, B.; Pischel, U., An Inhibit (INH) Molecular Logic Gate Based on 1,8-naphthalimide-sensitised Europium Luminescence. *Photochem. Photobiol. Sci.* **2004,** *3*, 639-642.
55. de Bettencourt-Dias, A.; Viswanathan, S.; Rollett, A., Thiophene-derivatized pybox and its highly luminescent lanthanide ion complexes. *J. Am. Chem. Soc.* **2007,** *129*, 15436-15437.
56. de Bettencourt-Dias, A.; Barber, P. S.; Viswanathan, S.; de Lill, D. T.; Rollett, A.; Ling, G.; Altun, S., *para*-Derivatized Pybox ligands as sensitizers in highly luminescent Ln(III) complexes. *Inorg. Chem.* **2010,** *49*, 8848-8861.
57. de Bettencourt-Dias, A., Introduction to Lanthanide Ion Luminescence. In *Luminescence of Lanthanide Ions in Coordination Compounds and Nanomaterials*, de Bettencourt-Dias, A., Ed. Wiley: 2014;
58. Dai, L.; Wu, D.; Qiao, Q.; Yin, W.; Yin, J.; Xu, Z., A naphthalimide-based fluorescent sensor for halogenated solvents. *Chem. Commun.* **2016,** *52*, 2095-2098.
59. Ventura, B.; Bertocco, A.; Braga, D.; Catalano, L.; d'Agostino, S.; Grepioni, F.; Taddei, P., Luminescence Properties of 1,8-Naphthalimide Derivatives in Solution, in Their Crystals, and in Co-crystals: Toward Room-Temperature Phosphorescence from Organic Materials. *J. Phys. Chem. C* **2014,** *118*, 18646-18658.
60. Middleton, R. W.; Parrick, J.; Clarke, E. D.; Wardman, P., Synthesis and fluorescence of N-substituted-1,8-naphthalimides. *J. Heterocycl. Chem.* **1986,** *23*, 849-855.
61. Carnall, W. T.; Fields, P. R.; Rajnak, K., Electronic Energy Levels of the Trivalent Lanthanide Aquo Ions. II. Gd3+. *J. Chem. Phys.* **1968,** *49*, 4443-4446.
62. Ko, C.-C.; Yam, V. W.-W., Coordination Compounds with Photochromic Ligands: Ready Tunability and Visible Light-Sensitized Photochromism. *Acc. Chem. Res.* **2018,** *51*, 149-159.
63. Crosby, G. A.; Whan, R. E.; Alire, R. M., Intramolecular Energy Transfer in Rare Earth Chelates. Role of the Triplet State. *J. Chem. Phys.* **1961,** *34* 743-748.
64. Renaud, F.; Piguet, C.; Bernardinelli, G.; Bünzli, J.-C. G.; Hopfgartner, G., In Search for Mononuclear Helical Lanthanide Building Blocks with Predetermined Properties:

Lanthanide Complexes with Diethyl Pyridine-2, 6-Dicarboxylate. *Chem.: Eur. J.* **1997,** *3*, 1660-1667.

65. Renaud, F.; Piguet, C.; Bernardinelli, G.; Bünzli, J.-C. G.; Hopfgartner, G., In Search for Mononuclear Helical Lanthanide Building Blocks with Predetermined Properties: Triple-stranded Helical Complexes with N,N,N',N'-tetraethylpyridine-2,6-dicarboxamide. *Chem.: Eur. J.* **1997,** *3*, 1646-1659.

66. Ridley, J. E.; Zerner, M. C., Triplet states via intermediate neglect of differential overlap: Benzene, pyridine and the diazines. *Theor. Chim. Acta* **1976,** *42*, 223-236.

67. Neese, F., The ORCA program system. *Wiley Interdiscip. Rev. Comput. Mol. Sci.* **2012,** *2*, 73-78.

68. Dutra, J. D. L.; Bispo, T. D.; Freire, R. O., LUMPAC lanthanide luminescence software: Efficient and user friendly. *J. Comput. Chem.* **2014,** *35*, 772-775.

69. Carnall, W. T., Fields, P. R., Wybourne, B. G., Electronic Energy Levels in the Trivalent Lanthanide Aquo Ions. I. Pr3+, Nd3+, Pm3+, Sm3+, Dy3+, Ho3+, Er3+, and Tm3+. *J. Chem. Phys.* **1968,** *49*, 4424.

70. Carnall, W. T.; Fields, P. R.; Rajnak, K., Electronic Energy Levels of the Trivalent Lanthanide Aquo Ions. IV. Eu3+. *J. Chem. Phys.* **1968,** *49*, 4450-4455.

71. Renaud, F.; Piguet, C.; Bernardinelli, G.; Bünzli, J.-C. G.; Hopfgartner, G., In Search for Mononuclear Helical Lanthanide Building Blocks with Predetermined Properties: Lanthanide Complexes with Diethyl Pyridine-2, 6-Dicarboxylate. *Chem.: Eur. J* **1997,** *3*, 1660-1667.

72. Luminescence of Lanthanide Ions in Coordination Compounds and Nanomaterials. de Bettencourt-Dias, A., Ed. John Wiley and Sons: 2014.

73. Bünzli, J.-C. G.; Choppin, G. R., *Lanthanide Probes in Life, Chemical and Earth Sciences - Theory and Practice*. Elsevier: Amsterdam, 1989.

74. Bünzli, J. C. G., Rare earth luminescent centers in organic and biochemical compounds. In *Spectroscopic Properties of Rare Earths in Optical Materials*, Liu, G.; Jacquier, B., Eds. Springer: Berlin, 2005; Vol. 83.

75. Freire, R. O.; Rocha, G. B.; Simas, A. M., Sparkle/PM3 for the modeling of europium(III), gadolinium(III), and terbium(III) complexes. *J Braz. Chem. Soc.* **2009,** *20*, 1638-1645.

76. Stewart, J. J. P., *MOPAC2016*. Stewart Computational Chemistry: Colorado Springs, 2016;

77. Monteiro, J. H. S. K.; de Bettencourt-Dias, A.; Sigoli, F. A., Estimating the Donor–Acceptor Distance To Tune the Emission Efficiency of Luminescent Lanthanide Compounds. *Inorg. Chem.* **2017,** *56*, 709-712.

78. Monteiro, J. H. S. K.; de Bettencourt-Dias, A.; Mazali, I. O.; Sigoli, F. A., The effect of 4-halogenobenzoate ligands on luminescent and structural properties of lanthanide complexes: experimental and theoretical approaches. *New Journal of Chemistry* **2015,** *39*, 1883-1891.

79. Latva, M.; Takalo, H.; Mukkala, V.-M.; Matachescu, C.; Rodríguez-Ubis, J. C.; Kankare, J., Correlation between the lowest triplet state energy level of the ligand and lanthanide(III) luminescence quantum yield. *J. Lumin.* **1997,** *75*, 149-169.
80. Bettencourt-Dias, A. d., *Luminescence of Lanthanide Ions in Coordination Compounds and Nanomaterials*. John Wiley & Sons, Ltd.: Chichester, United Kingdom, 2014;
81. Fernandez, J. M.; Bilgin, M. D.; Grossweiner, L. I., Singlet Oxygen Generation by Photodynamic Agents. *J. Photochem. Photobio. B* **1997,** *37*, 131-140.
82. Dai, R.; Shoemaker, R.; Farrens, D.; Han, M. J.; Kim, C. S.; Song, P.-S., Characterization of Silkworm Chlorophyll Metabolites as an Active Photosensitizer for Photodynamic Therapy. *J. Nat. Prod.* **1992,** *55*, 1241-1251.
83. Chacon, J. N.; McLearie, J.; Sinclair, R. S., Singlet Oxygen Yields and Radical Contributions in the Dye-Sensitized Photooxidation in Methanol of Esters of Polyunsaturated Fatty Acids (Oleic, Linoleic, Linolenic, and Arachionic). *Photochem. Photobiol.* **1988,** *47*, 647-656.
84. Sessler, J. L.; Dow, W. C.; O'Connor, D.; Harriman, A.; Hemmi, G.; Mody, T. D.; Miller, R. A.; Qing, F.; Springs, S.; Woodburn, K.; Young, S. W., Biomedical applications of lanthanide (III) texaphyrins Lutetium(III) texaphyrins as potential photodynamic therapy photosensitizers. *J. Alloys Compd.* **1997,** *249*, 146-152.
85. Bassett, J.; Denney, R. C.; Jeffery, G. H.; Mendham, J., In *Vogel's Textbook of Quantitative Inorganic Analysis*, 4th ed.; Longman Group: London, U.K., 1978;
86. Gans, P.; Sabatini, A.; Vacca, A., Investigation of equilibria in solution. Determination of equilibrium constants with the HYPERQUAD suite of programs. *Talanta* **1996,** *43*, 1739-1753.
87. Alderighi, L.; Gans, P.; Ienco, A.; Peters, D.; Sabatini, A.; Vacca, A., Hyperquad simulation and speciation (HySS): a utility program for the investigation of equilibria involving soluble and partially soluble species. *Coord. Chem. Rev.* **1999,** *184*, 311-318.
88. Hänninen, P. H., H., *Lanthanide Luminescence Photophysical, Analytical and Biological Aspects*. 1 ed.; Springer-Verlag Berlin Heidelberg: 2011;
89. Melhuish, W. H., Quantum efficiencies of fluorescence of organic substances: Effect of solvent and concentration of the fluorescent solute. *J. Phys. Chem.* **1961,** *65*, 229-235.
90. Chauvin, A. S.; Gumy, F.; Imbert, D.; Bünzli, J. C. G., Europium and Terbiumtris(Dipicolinates) as Secondary Standards for Quantum Yield Determination. *Spectrosc. Lett.* **2004,** *37*, 517-532.
91. Chauvin, A.-S.; Gumy, F.; Imbert, D.; Bünzli, J.-C. G., Europium and Terbium tris(Dipicolinates) as Secondary Standards for Quantum Yield Determination. [Erratum to document cited in CA142:489604]. *Spectroscopy Lett.* **2007,** *40*, 193.
92. Becker, R. S.; Seixas de Melo, J.; Maçanita, A. L.; Elisei, F., Comprehensive Evaluation of the Absorption, Photophysical, Energy Transfer, Structural, and Theoretical

Properties of α-Oligothiophenes with One to Seven Rings. *J. Phys. Chem.* **1996,** *100*, 18683-18695.
93. Marles Robin, J.; Hudson James, B.; Graham Elizabeth, A.; Soucy-Breau, C.; Morand, P.; Compadre, R. L.; Compadre Cesar, M.; Towers, G. H. N.; Arnason, J. T., Structure-activity studies of photoactivated antiviral and cytotoxic tricyclic thiophenes. . *Photochem. Photobiol.* **1992,** *56*, 479-487.
94. Sato, T.; Hamada, Y.; Sumikawa, M.; Araki, S.; Yamamoto, H., Solubility of Oxygen in Organic Solvents and Calculation of the Hansen Solubility Parameters of Oxygen. *Ind. Eng. Chem. Res.* **2014,** *53*, 19331-19337.
95. Manring, L. E.; Foote, C. S., Chemistry of singlet oxygen. 44. Mechanism of photooxidation of 2,5-dimethylhexa-2,4-diene and 2-methyl-2-pentene. *J. Am. Chem. Soc.* **1983,** *105*, 4710-4717.
96. Scaiano, J. C.; Redmond, R. W.; Mehta, B.; Arnason, J. T., Efficiency of the photoprocesses leading to singlet oxygen (1δg) generation by α-terthienyl: otical absorption, optoacoustic calorimetry and infrared luminescence studies. *Photochem. Photobiol.* **1990,** *52*, 655-659.
97. Ciofalo, M.; Ponterini, G., Generation of singlet oxygen by 2,2′:5′,2″-terthiophene and some of its derivatives. *J. Photochem. Photobio. A* **1994,** *83*, 1-6.
98. Aebischer, A.; Gumy, F.; Bünzli, J.-C. G., Intrinsic quantum yields and radiative lifetimes of lanthanide tris(dipicolinates). *Phys. Chem. Chem. Phys.* **2009,** *11*, 1346-1353.
99. de Sá, G. F.; Malta, O. L.; de Mello Donegá, C.; Simas, A. M.; Longo, R. L.; Santa-Cruz, P. A.; da Silva, E. F., Spectroscopic properties and design of highly luminescent lanthanide coordination complexes. *Coord. Chem. Rev.* **2000,** *196*, 165-195.
100. Tsierkezos, N. G., Electron transfer kinetics for the cobaltocene (+1/0) couple at platinum disk electrode in acetonitrile/dichloromethane binary solvent system. *J. Mol. Liq.* **2008,** *138*, 1-8.
101. de Andrade, A. V. M.; da Costa, N. B.; Simas, A. M.; de Sá, G. F., Sparkle model for the quantum chemical AM1 calculation of europium complexes. *Chem. Phys. Lett.* **1994,** *227*, 349-353.

SYNOPSIS

1,8-Naphthalimide-based lanthanide ion complexes were isolated and their properties as metal-centered emitters and singlet oxygen generators explored. These compounds display red Eu^{III} emission with efficiencies up to 17%, and weaker NIR Nd^{III} and Yb^{III} emission. Singlet oxygen generation efficiencies are as high as 64%. These values are higher in an oxygen-free environment, confirming the competitive relationship between metal-centered emission and singlet oxygen generation, as both processes involve the ligand's triplet state.

TOC Graphic